12-2015

Predicted Stresses in a Ball-Grid-Array (BGA)/Column-Grid-Array (CGA) Assembly With a Low Modulus Solder at its Ends

Ephraim Suhir
Portland State University

Reza Ghaffarian
Jet Propulsion Laboratory

Citation Details

Ephraim, S. and Ghaffarian, R. (2015). Predicted Stresses in a Ball-Grid-Array (BGA)/Column-Grid-Array (CGA) Assembly with a Low Modulus Solder at its Ends. Journal of Materials Science: Materials in Electronics, Volume 26, Issue 12, pp 9680-9688.

J Mater Sci: Mater Electron (2015) 26:9680–9688
DOI 10.1007/s10854-015-3635-6

Predicted stresses in a ball-grid-array (BGA)/column-grid-array (CGA) assembly with a low modulus solder at its ends

Ephraim Suhir[1,2,3] · **Reza Ghaffarian**[4]

Published online: 4 September 2015

Abstract A simple, easy-to-use and physically meaningful predictive model is suggested for the assessment of thermal stresses in a ball-grid-array or a column-grid-array with a low modulus solder material at the peripheral portions of the assembly. It is shown that the application of such a design can lead to a considerable relief in the interfacial stresses, even to an extent that inelastic strains in the solder joints could be avoided. If this happens, the fatigue strength of the bond and of the assembly as a whole will be improved dramatically: low-cycle fatigue conditions will be replaced by the elastic fatigue condition, and Palmgren–Minor rule of linear accumulation of damages could be used instead of one of the numerous Coffin–Manson models to assess the lifetime of the material.

1 Introduction

Bonded assemblies (joints) subjected to thermal and/or mechanical loading are widely used in engineering, including the fields of electronics, optoelectronics and photonics. The most reliable adhesively bonded or soldered assemblies are characterized by stiff adherends and a compliant bonding layer. This circumstance is well known from the engineering practice [1–10] and has been confirmed by modeling, both analytical and computer-aided, and experimentation [11–50].

Low modulus and relatively thick (up to 4 mils or even thicker) bonding layers where employed to provide an effective strain buffer between the bonded components [51–54]. But still, because of the stress concentration at the assembly ends, the induced stresses and especially the interfacial shearing and peeling stresses, are often much higher than acceptable for many applications. This is particularly true for ball-grid and pad-grid array structures, in which the "bonding" layer is only moderately compliant. Solder materials are prone to inelastic deformations. This shortens considerably their fatigue life-time. There exists therefore a crucial need for a reduction in the interfacial shearing stresses in bonded assemblies and particularly in solder joint interconnections.

Some assemblies with an inhomogeneous bonding layer, when only the assembly ends were bonded, were considered [55–60], with an emphasis on the interaction of the "local" and "global" thermal expansion (contraction) mismatch stresses. The "global" stresses in the bond are due to the mismatch of the bonded materials outside the bonded area, while the "local" mismatch results in stresses within this area. It has been found that this interaction is such that the "global" and the "local" interfacial stresses should be summed up for the end cross-sections of the assembly, but compensate each other, to a greater or lesser extent, at the inner edges of the bonding joint. It has been found also that if the end bonds are sufficiently long and/or stiff, the states of stress and strain in the mid-portion of the assembly will not be different of those in a "conventional" assembly, where the bonding material occupies the entire area between the assembly components. This finding is particularly important for assemblies with underfills: the

✉ Ephraim Suhir
suhire@aol.com; e.suhir@ieee.org;
http://www.ERSuhir.com

[1] Portland State University, Portland, OR, USA

[2] Technical University, Vienna, Austria

[3] ERS Co., 727 Alvina Ct., Los Altos, CA 94024, USA

[4] Jet Propulsion Laboratory (JPL), California Institute of Technology, Pasadena, CA, USA

solder joints in the mid-portion of the assembly will still experience low stresses. These stresses might be even lower than in an assembly with an underfill material placed under the entire area between the adherends, because the solder joints will not be subjected to stresses due to the mismatch between the underfill and the solder materials.

Various assemblies with inhomogeneous bonding layers were addressed in application to the predicted size of an inelastic zone in ball-grid-array (BGA) assemblies [61], to the problem of stress minimization in thermo-electric module designs [62], and for the explanation of a paradoxical situation, when stiffer mid-portions of compliant bonds could result in appreciably lower stresses at the assembly ends [63]. Identical bonded components and "piecewise-continuous" bonding layer were considered in application to a new generation of low cost memory storages, in which the bonding layer played the role of the memory storing medium [64–66]. The emphasis was on the conditions that could lead to plane boundaries between the "pieces" of the bonding layer, rather than to low level stresses.

In this analysis a simple, easy-to-use and physically meaningful predictive analytical model is suggested for the evaluation of the interfacial shearing stresses in an electronic packaging assembly with a BGA or a column-grid-array (CGA) bonding system with a low modulus bonding material at the ends. The analysis is, in effect, a modification and an extension, for the case of the BGA/CGA interconnects, of the models suggested earlier [57–59] for adhesively bonded assemblies. The analysis is limited, to the interfacial shearing stresses, i.e., does not address the peeling stresses. This is considered as a future work, as well as finite-element analysis predictions.

2 Analysis

2.1 Mid-portion of the assembly

Consider first a bonded assembly comprised of dissimilar materials, experiencing the change in temperature and subjected to thus far unknown external forces $\hat{T}$ applied to the assembly components in a symmetric fashion (Fig. 1).

The interfacial longitudinal displacements of the assembly components can be sought, in an approximate analysis, using the concept of the interfacial compliances [15, 16], as follows:

$$\left.\begin{aligned} u_1(x) &= -\alpha_1 \Delta t x + \lambda_1 \int_0^x T(\xi)d\xi - \kappa_1 \tau(x) - \frac{h_1}{2} w_1'(x) \\ u_2(x) &= -\alpha_2 \Delta t x - \lambda_2 \int_0^x T(\xi)d\xi + \kappa_2 \tau(x) + \frac{h_2}{2} w_2'(x) \end{aligned}\right\}. \tag{1}$$

Here α_1 and α_2 are the coefficients of thermal expansion (CTE) of the component materials, Δt is the change in temperature,

$$\lambda_1 = \frac{1-\nu_1}{E_1 h_1}, \quad \lambda_2 = \frac{1-\nu_2}{E_2 h_2} \tag{2}$$

are the axial compliances of the components, h_1 and h_2 are their thicknesses, E_1 and E_2 are Young's moduli of the materials, ν_1 and ν_2 are Poisson's ratios,

$$T(x) = \int_{-l}^{x} \tau(\xi)d\xi + \hat{T} \tag{3}$$

are the distributed forces acting in the x cross-section, $\tau(x)$ is the interfacial shearing stress, $\hat{T}$ is the force applied from the peripheral portions of the assembly, l is half the assembly length, κ_1 and κ_2 are the interfacial compliances of the assembly components, and $w_1(x)$ and $w_2(x)$ are the component deflections. The origin of the coordinate x is in the mid-cross-section of the assembly.

The first terms in (1) are stress-free thermal contractions. The second terms determine the displacements due to the induced thermal forces and are evaluated in accordance with the Hooke's law. The third terms are corrections that account for the fact that the interfacial displacements are somewhat larger than the displacements of the inner points of the given cross-section. It is assumed that these corrections can be evaluated as the product of the interfacial compliances [16]

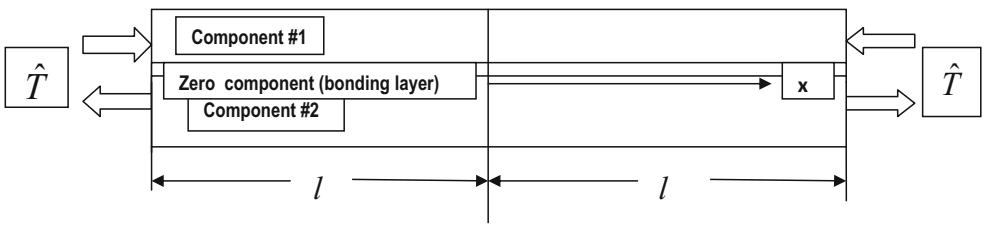

Fig. 1 This structure represents the mid-portion of a bonded bi-material assembly subjected to thermal loading, because of the change in temperature and thermal expansion/contraction mismatch of the dissimilar materials of the components #1 and #2, as well as to the mechanical loading from the peripheral portions of the assembly

$$\kappa_1 = \frac{h_1}{3G_1}, \quad \kappa_2 = \frac{h_2}{3G_2} \tag{4}$$

of the bonded components and the interfacial shearing stress acting in this cross-section. In these formulas

$$G_1 = \frac{E_1}{2(1+\nu_1)}, \quad G_2 = \frac{E_2}{2(1+\nu_2)}, \tag{5}$$

are the shear moduli of the materials. The forth terms in (1) are due to bending. Since the case of cooling is considered here, and the CTE of the component #1 is lower than that of the component #2, the interfacial surface of the component #1 is configured in the concave fashion and the surface of the component #2 is configured in the convex fashion. This circumstance is reflected by the signs in front of the corresponding terms.

The condition of the compatibility of the displacements (1) can be written as

$$u_1(x) = u_2(x) - \kappa_0 \tau(x) \tag{6}$$

where κ_0 is the longitudinal interfacial compliance of the bonding layer. The second term in the right part of this condition is due to the interfacial compliance of the bond. This compliance can be evaluated as

$$\kappa_0 = \frac{h_0}{G_0}, \tag{7}$$

where

$$G_0 = \frac{E_0}{2(1+\nu_0)} \tag{8}$$

is the shear modulus of the bonding material.

Introducing the formulas (1) into the condition (6) we obtain:

$$\kappa\tau(x) - (\lambda_1+\lambda_2) \int_0^x T(\xi)d\xi - \frac{h_1}{2}w_1'(x) - \frac{h_2}{2}w_2'(x) = \Delta\alpha\Delta t x. \tag{9}$$

Here $\kappa = \kappa_0 + \kappa_1 + \kappa_2$ is the total interfacial compliance of the assembly, and $\Delta\alpha = \alpha_2 - \alpha_1$ is the thermal expansion (contraction) mismatch of the components' materials.

By differentiating the Eq. (9) with respect to the coordinate x we find:

$$\kappa\tau'(x) - (\lambda_1+\lambda_2)T(x) - \frac{h_1}{2}w_1''(x) - \frac{h_2}{2}w_2''(x) = \Delta\alpha\Delta t \tag{10}$$

The curvatures $w_1''(x)$ and $w_2''(x)$ can be determined from the equilibrium equations

$$\begin{aligned} D_1 w_1''(x) &= -\frac{h_1}{2}T(x) - \int_{-l}^{x}\int_{-l}^{x} p(\xi)d\xi d\xi, \\ D_2 w_2''(x) &= -\frac{h_2}{2}T(x) + \int_{-l}^{x}\int_{-l}^{x} p(\xi)d\xi d\xi, \end{aligned} \tag{11}$$

for the assembly components as follows:

$$\begin{aligned} w_1''(x) &= -\frac{h_1}{2D_1}T(x) - \frac{1}{D_1}\int_{-l}^{x}\int_{-l}^{x} p(\xi)d\xi d\xi, \\ w_2''(x) &= -\frac{h_2}{2D_2}T(x) + \frac{1}{D_2}\int_{-l}^{x}\int_{-l}^{x} p(\xi)d\xi d\xi, \end{aligned} \tag{12}$$

In the Eqs. (11),

$$D_1 = \frac{E_1 h_1^3}{12(1-\nu_1^2)}, \quad D_2 = \frac{E_2 h_2^3}{12(1-\nu_2^2)}, \tag{13}$$

are the flexural rigidities of the assembly components treated as elongated rectangular plates, and $p(x)$ is the peeling stress. The left parts of the Eqs. (11) are elastic bending moments. The first terms in the right parts are the bending moments caused by the forces $T(x)$ and the second terms are the bending moments caused by the peeling stress $p(x)$.

Introducing the expressions (12) for the curvatures into the Eq. (10) we obtain:

$$\kappa\tau'(x) - \lambda T(x) + \mu\int_{-l}^{x}\int_{-l}^{x} p(\xi)d\xi d\xi = \Delta\alpha\Delta t \tag{14}$$

where

$$\lambda = \lambda_1 + \lambda_2 + \frac{h_1^2}{4D_1} + \frac{h_2^2}{4D_2} \tag{15}$$

is the axial compliance of the assembly with consideration of the effect of bending, and

$$\mu = \frac{h_1}{2D_1} - \frac{h_2}{2D_2} \tag{16}$$

is the factor that considers the role of the dissimilar components' flexural rigidity and its effect on the peeling stress. In an approximate analysis the effect of the peeling stress on the interfacial shearing stress need not be accounted for, and the Eq. (14) can be replaced by the simplified equation:

$$\kappa\tau'(x) - \lambda T(x) = \Delta\alpha\Delta t, \tag{17}$$

in which the shearing stress only is considered.

The force $T(x)$ should be symmetric with respect to the mid-cross-section of the assembly and could be sought as

$$T(x) = C_0 + C_2 \cosh kx \tag{18}$$

Introducing this solution into the Eq. (17) and considering that, in accordance with the formula (3),

$$\tau'(x) = T''(x) = k^2 C_2 \cosh kx, \tag{19}$$

we conclude that the Eq. (17) is fulfilled, if the following relationships

$$k = \sqrt{\frac{\lambda}{\kappa}}, \quad C_0 = -\frac{\Delta\alpha\Delta t}{\lambda} \tag{20}$$

take place. As to the constant C_2 of integration in the solution (18), it can be found from the boundary condition

$$T(\pm l) = \hat{T} \tag{21}$$

for the thermally induced force $T(x)$ as follows:

$$C_2 = \left(\frac{\Delta\alpha\Delta t}{\lambda} + \hat{T}\right)\frac{1}{\cosh kl} \tag{22}$$

Then the solution (18) results in the following expression for the induced force:

$$T(x) = -\frac{\Delta\alpha\Delta t}{\lambda}\left(1 - \frac{\cosh kx}{\cosh kl}\right) + \hat{T}\frac{\cosh kx}{\cosh kl} \tag{23}$$

The first term in this expression is due to the thermal mismatch of the assembly components and the second term is caused by the thus far unknown external "mechanical" force applied from the peripheral portions of the assembly.

The interfacial shearing stress can be found from (23) by differentiation:

$$\tau(x) = T'(x) = k\left(\frac{\Delta\alpha\Delta t}{\lambda} + \hat{T}\right)\frac{\sinh kx}{\cosh kl} \tag{24}$$

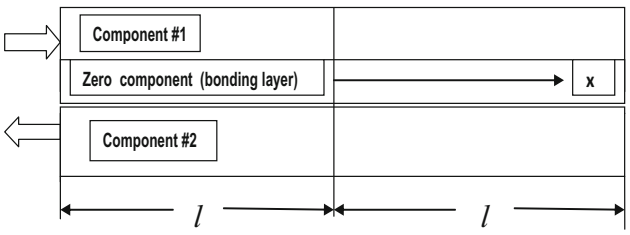

Fig. 2 This structure represents the peripheral portion of a bonded bi-material assembly subjected to thermal loading, because of the change in temperature and thermal expansion/contraction mismatch of the dissimilar materials of the components #1 and #2, as well as to the mechanical loading from the mid-portion of the assembly

2.2 Peripheral portion of the assembly

Consider now the peripheral portion of the assembly (Fig. 2). Unlike the mid-portion, the peripheral portion is subjected to the mechanical loading applied to only one side of the assembly.

The Eq. (17) is still applicable, but the boundary conditions for the induced forces are different:

$$T(-l) = \hat{T}, \quad T(l) = 0. \tag{25}$$

In order to satisfy these two boundary conditions, the induced force should be sought in the form

$$T(x) = C_0 + C_1 \sinh kx + C_2 \cosh kx \tag{26}$$

that contains two constants of integration and is not symmetric anymore with respect to the mid-cross-section of the peripheral portion. Introducing the sought solution (26) into the equation (17), we find that the formulas (20) are still valid, but the constants of integration are expressed as follows:

$$C_1 = -\frac{\hat{T}}{2\sinh kl}, \quad C_2 = \left(\frac{\Delta\alpha\Delta t}{\lambda} + \frac{\hat{T}}{2}\right)\frac{1}{\cosh kl}. \tag{27}$$

Introducing the second formula in (20) and the formulas (27) into the solution (26), we obtain the following expression for the induced force:

$$T(x) = -\frac{\Delta\alpha\Delta t}{\lambda}\left(1 - \frac{\cosh kx}{\cosh kl}\right) + \hat{T}\frac{\sinh[k(l-x)]}{\sinh 2kl} \tag{28}$$

The first ("thermal") term in the obtained expression for the induced force is not different of the first term in (23), but the second term is quite different, because of the different "mechanical" loading. The interfacial shearing stress can be found by differentiation:

$$\tau(x) = T'(x) = k\left[\frac{\Delta\alpha\Delta t}{\lambda}\frac{\sinh kx}{\cosh kl} - \hat{T}\frac{\cosh[k(l-x)]}{\sinh 2kl}\right] \tag{29}$$

2.3 Thermal force at the boundary of the mid-portion and the peripheral portions

The force $\hat{T}$ at the boundary between the mid-portion and the peripheral portions of the assembly can be determined from the condition of the compatibility of the longitudinal interfacial displacements of the mid-portion and the peripheral portions of the assembly at their boundary.

The formulas (24) and (29) yield:

$$\tau(L-2l) = K\left(\frac{\Delta\alpha\Delta t}{\lambda} + \hat{T}\right)\tanh[K(L-2l)],$$
$$\tau(-l) = -k\left(\frac{\Delta\alpha\Delta t}{\lambda}\tanh kl + \hat{T}\coth 2kl\right), \tag{30}$$

where the notation in the first formula has been changed to account, because for the possibly different parameter of the interfacial shearing stress (K instead of k) and because half the length $L - 2l$ of the mid-portion can be found as the difference between half the assembly length L and the length $2l$ of one of the peripheral portions. Since the interfacial displacements can be found as products of the interfacial compliances and the interfacial shearing stresses, the condition of the compatibility of the interfacial displacements of the mid-portion and the peripheral portion of the assembly at their boundary can be written as follows:

$$K\kappa_m\left(\frac{\Delta\alpha\Delta t}{\lambda}+\hat{T}\right)\tanh[K(L-2l)] = -k\kappa_p\left(\frac{\Delta\alpha\Delta t}{\lambda}\tanh kl+\hat{T}\coth 2kl\right) \tag{31}$$

Considering that, in accordance with the first formula in (20), $\kappa_m = \frac{\lambda}{K^2}$ and $\kappa_p = \frac{\lambda}{k^2}$, and solving the Eq. (31) for the force $\hat{T}$, we obtain:

$$\hat{T} = -\frac{\Delta\alpha\Delta t}{\lambda}\frac{\eta\tanh[K(L-2l)]+\tanh kl}{\eta\tanh[K(L-2l)]+\coth 2kl}, \tag{32}$$

where $\eta = \frac{k}{K}$ is the ratio of the parameters of the interfacial shearing stress at the peripheral portion and at the mid-portion of the assembly.

For long and/or stiff mid-portions, which is usually the case in actual structures, the obtained formula can be simplified:

$$\hat{T} = -\frac{\Delta\alpha\Delta t}{\lambda}\frac{\eta+\tanh kl}{\eta+\coth 2kl}. \tag{33}$$

For long enough peripheral portions this formula yields: $\hat{T} = -\frac{\Delta\alpha\Delta t}{\lambda}$.

2.4 Interfacial stresses

Introducing (32) into the formulas (30) for the stresses acting at the boundary of the two assembly portions we obtain:

$$\tau_m(L-2l) = K\frac{\Delta\alpha\Delta t}{\lambda}\frac{\coth 2kl-\tanh kl}{\eta+\coth[K(L-2l)]\coth 2kl}, \tag{34}$$

$$\tau_p(-l) = k\frac{\Delta\alpha\Delta t}{\lambda}\frac{\eta}{\eta\sinh 2kl+\coth[K(L-2l)]\cosh 2kl}. \tag{35}$$

In the special case of a homogeneous bonding layer, when $K = k$ and $\eta = 1$, the above two formulas yield

$$\tau(L-2l) = \tau(-l) = k\frac{\Delta\alpha\Delta t}{\lambda}\frac{\sinh[k(L-2l)]}{\cosh kL}, \tag{36}$$

as it is supposed to be. From (29), with consideration of the expression (32) for the force at the boundary, we find:

$$\tau_p(l) = k\frac{\Delta\alpha\Delta t}{\lambda}\frac{\eta\tanh[K(L-2l)]\cosh 2kl+\sinh 2kl}{\eta\tanh[K(L-2l)]\sinh 2kl+\cosh 2kl}. \tag{37}$$

In the typical case of a stiff-and-long mid-portion the formulas (34), (35) and (37) can be simplified:

$$\tau_m(L-2l) = K\frac{\Delta\alpha\Delta t}{\lambda}\frac{\coth 2kl-\tanh kl}{\eta+\coth 2kl}, \tag{38}$$

$$\tau_p(-l) = k\frac{\Delta\alpha\Delta t}{\lambda}\frac{\eta}{\eta\sinh 2kl+\cosh 2kl}, \quad \tau_p(l) = k\frac{\Delta\alpha\Delta t}{\lambda}\frac{\eta+\tanh 2kl}{1+\eta\tanh 2kl}. \tag{39}$$

For long peripheral portions, these formulas yield:

$$\tau_m(L-2l)\approx 0, \tau_p(-l)\approx 0, \tau_p(l) = k\frac{\Delta\alpha\Delta t}{\lambda}. \tag{40}$$

In the case of a homogeneous bonding layer, when $K = k$ and $\eta = 1$, the formula (37) yields:

$$\tau_p(l) = k\frac{\Delta\alpha\Delta t}{\lambda}\tanh kL. \tag{41}$$

This is a well known result.

3 Numerical example

The numerical example is carried out for a typical package (component #1)/PCB (component #2) assembly with either BGA or CGA solder joint interconnections. The solder material in the mid-portion has an appreciably higher Young's modulus that the one at the peripheral portions.

3.1 Input data

Structural element	Package	PCB	Solder the assembly mid-portion 3–4 %Ag0.5–1 %Cu	Solder at the assembly ends Sn96.5Ag3.5
Element number	1 and 3	2	12 and 23	12 and 23
Young's modulus, E (kg/mm^2)	8775.5	2321.4	5510.0	2670.0
Poisson's ratio, v	0.25	0.40	0.35	0.35
CTEα, 1/°C	6.5×10^{-6}	15.0×10^{-6}	x	x
Thickness, h (mm)	2.0	1.5	0.60/BGA	0.60/BGA
			2.20/CGA	2.20/CGA
Shear modulus, G (kg/mm^2)	3367.3	892.7	2040.7	990.1
Axial compliance, λ (mm/kg)	3.9884×10^{-5}	20.1028×10^{-5}	x	x
Interfacial compliance, κ (mm^3/kg)	19.7982×10^{-5}	56.0099×10^{-5}	29.4017×10^{-5}/BGA	29.4017×10^{-5}/BGA
			107.8061×10^{-5}/CGA	107.8061×10^{-5}/CGA
Flexural rigidity, D (kg mm)	6240.3556	777.2545	–	–

Estimated yield stress of the solder material in shear: $\tau_Y = 1.85\,\text{kgf/mm}^2$ for the solder in mid-portion and $\tau_Y = 1.35\,\text{kgf/mm}^2$ for the solder at peripheral portions; Temperature change $\Delta t = 200$ °C; Half assembly length $L = 15$ mm; Lengths the peripheral zones $2l = 2.0$ mm; Thermally induced force in the mid-portion of the assembly $\frac{\Delta\alpha\Delta t}{\lambda_*} = \frac{0.0017}{72.3701 \times 10^{-5}} = 2.3490\,\text{kg/mm}$.

3.2 Calculated data

3.2.1 Axial compliances

$$\lambda_1 = \frac{1 - v_1}{E_1 h_1} = \frac{1 - 0.3}{8775.5 \times 2.0} = 3.9884 \times 10^{-5}\,\text{mm/kg};$$

$$\lambda_2 = \frac{1 - v_2}{E_2 h_2} = \frac{1 - 0.3}{2321.4 \times 1.5} = 20.1028 \times 10^{-5}\,\text{mm/kg};$$

$$\lambda = \lambda_1 + \lambda_2 = 24.0912 \times 10^{-5}\,\text{mm/kg};$$

Interfacial compliances of the components:

$$\kappa_1 = \frac{h_1}{3G_1} = \frac{2.0}{3 \times 3367.3} = 19.7983 \times 10^{-5}\,\text{mm}^3/\text{kg},$$

$$\kappa_2 = \frac{h_2}{3G_2} = \frac{1.5}{3 \times 892.7} = 56.0100 \times 10^{-5}\,\text{mm}^3/\text{kg}$$

Interfacial compliances for solders in the mid-portion of the assembly:

$$\kappa_0 = \frac{h_0}{G_0} = \frac{0.6}{2040.7} = 29.4017 \times 10^{-5}\,\text{mm}^3/\text{kg}$$

in the case of BGA, and

$$\kappa_0 = \frac{h_0}{G_0} = \frac{2.2}{2040.7} = 107.8061 \times 10^{-5}\,\text{mm}^3/\text{kg}$$

in the case of for CGA.

Interfacial compliances for solders at the peripheral portions of the assembly:

$$\kappa_0 = \frac{h_0}{G_0} = \frac{0.6}{990.1} = 60.6000 \times 10^{-5}\,\text{mm}^3/\text{kg}$$

in the case of BGA, and

$$\kappa_0 = \frac{h_0}{G_0} = \frac{2.2}{990.1} = 222.2000 \times 10^{-5}\,\text{mm}^3/\text{kg}$$

in the case of for CGA.

Then the total interfacial compliance at the mid-portion of the assembly is

$$\kappa = \kappa_0 + \kappa_1 + \kappa_2 = 105.2100 \times 10^{-5}\,\text{mm}^3/\text{kg}$$

in the case of BGA, and

$$\kappa = \kappa_0 + \kappa_1 + \kappa_2 = 183.6144 \times 10^{-5}\,\text{mm}^3/\text{kg}$$

in the case of CGA.

The total interfacial compliance at the peripheral portions of the assembly is

$$\kappa = \kappa_0 + \kappa_1 + \kappa_2 = 136.4088 \times 10^{-5}\,\text{mm}^3/\text{kg}$$

in the case of BGA, and

$$\kappa = \kappa_0 + \kappa_1 + \kappa_2 = 298.0083 \times 10^{-5}\,\text{mm}^3/\text{kg}$$

in the case of CGA.

The flexural rigidities of the assembly components are

$$D_1 = \frac{E_1 h_1^3}{12(1 - v_1^2)} = \frac{8775.5 \times 2.0^3}{12(1 - 0.25^2)} = 6240.3556\,\text{kg mm}$$

$$D_2 = \frac{E_2 h_2^3}{12(1 - v_2^2)} = \frac{2321.4 \times 1.5^3}{12(1 - 0.40^2)} = 777.2545\,\text{kg mm}$$

Total axial compliance is

$$\lambda_* = \lambda + \frac{h_1^2}{4D_1} + \frac{h_2^2}{4D_2} = 24.0912 \times 10^{-5} + \frac{2.0^2}{4 \times 6240.3556} + \frac{1.5^2}{4 \times 777.2545} = 72.3701 \times 10^{-5}\,\text{mm/kg}$$

The total axial compliance with consideration of bending is by the factor of three larger than the compliance of a bow-free assembly, so that the additional compliance due to the finite flexural rigidities of the assembly components should always be considered, when the shearing stress is evaluated.

The parameter of the interfacial shearing stress in the mid-portion of the assembly is

$$K = \sqrt{\frac{\lambda_*}{\kappa}} = \sqrt{\frac{72.3701 \times 10^{-5}}{105.2100 \times 10^{-5}}} = 0.8294\,\text{mm}^{-1}$$

in the case of BGA, and

$$K = \sqrt{\frac{\lambda_*}{\kappa}} = \sqrt{\frac{72.3701 \times 10^{-5}}{183.6144 \times 10^{-5}}} = 0.6278\,\text{mm}^{-1}$$

in the case of CGA. The parameter of the interfacial shearing stress for the peripheral portions of the assembly is

$$k = \sqrt{\frac{\lambda_*}{\kappa}} = \sqrt{\frac{72.3701 \times 10^{-5}}{136.4088 \times 10^{-5}}} = 0.7284\,\text{mm}^{-1}$$

in the case of BGA, and

$$k = \sqrt{\frac{\lambda_*}{\kappa}} = \sqrt{\frac{72.3701 \times 10^{-5}}{298.0083 \times 10^{-5}}} = 0.4928\,\text{mm}^{-1}$$

in the case of CGA. The ratio of the two above parameters of the interfacial shearing stress is

$$\eta = \frac{k}{K} = \frac{0.7284}{0.8294} = 0.8782\,\text{mm}^{-1}$$

in the case of BGA, and

$$\eta = \frac{k}{K} = \frac{0.4928}{0.6278} = 0.7850\,\text{mm}^{-1}$$

in the case of CGA.

The force at the boundary between the mid-portion and the peripheral portions of the assembly is

$$\hat{T} \approx -\frac{\Delta\alpha\Delta t}{\lambda}\frac{\eta + \tanh kl}{\eta + \coth 2kl} = -2.3490 \times \frac{0.8782 + 0.6221}{0.8782 + 1.6075} = -2.4964\,\text{kg/mm}$$

in the case of BGA, and

$$\hat{T} \approx -\frac{\Delta\alpha\Delta t}{\lambda}\frac{\eta + \tanh kl}{\eta + \coth 2kl} = -2.3490 \times \frac{0.7850 + 0.4564}{0.7850 + 2.1909} = -0.9799\,\text{kg/mm}$$

in the case of CGA.

Thus, the application of CGA system resulted in about 60 % reduction in the thermal force at the boundary of the mid-portion and the peripheral portions of the assembly.

The interfacial shearing stress in the assembly mid-portion at its boundary with the peripheral portion is

$$\tau_m(L - 2l) \approx K\left(\frac{\Delta\alpha\Delta t}{\lambda} + \hat{T}\right) = 0.8294(2.3490 - 2.9436) = -0.4932\,\text{kg/mm}^2$$

in the case of BGA, and is somewhat lower,

$$\tau_m(L - 2l) \approx K\left(\frac{\Delta\alpha\Delta t}{\lambda} + \hat{T}\right) = 0.6278(2.3490 - 2.9436) = -0.3733\,\text{kg/mm}^2,$$

in the case of CGA.

The interfacial shearing stress in the peripheral portions of the assembly at their boundaries with the mid-portion is

$$\tau_p(-l) = k\frac{\Delta\alpha\Delta t}{\lambda}\frac{\eta}{\eta\sinh 2kl + \cosh 2kl} = 0.7284 \times 2.3490\frac{0.8782}{0.8782 \times 2.0296 + 2.2626} = 0.3715\,\text{kg/mm}^2$$

in the case of BGA, and

$$\tau_p(-l) = k\frac{\Delta\alpha\Delta t}{\lambda}\frac{\eta}{\eta\sinh 2kl + \cosh 2kl} = 0.4928 \times 2.3490\frac{0.7850}{0.7850 \times 1.1531 + 1.5263} = 0.3737\,\text{kg/mm}^2$$

in the case of CGA.

The interfacial shearing stress is still the highest at the assembly ends and is

$$\tau_p(l) = k\frac{\Delta\alpha\Delta t}{\lambda}\frac{\eta + \tanh 2kl}{1 + \eta\tanh 2kl} = 0.7284 \times 2.3490\frac{0.8782 + 0.8970}{1 + 0.8782 \times 0.8970} = 1.6990\,\text{kg/mm}^2$$

in the case of BGA, and

$$\tau_p(l) = k\frac{\Delta\alpha\Delta t}{\lambda}\frac{\eta + \tanh 2kl}{1 + \eta\tanh 2kl} = 0.4928 \times 2.3490\frac{0.7850 + 0.7555}{1 + 0.7850 \times 0.7555} = 1.1194\,\text{kg/mm}^2$$

in the case of CGA.

When a homogeneous bonding layer with the characteristics of the mid-portion in the carried out example were used, the maximum interfacial shearing stress would be

$$\tau_{\max} = k_* \frac{\Delta\alpha\Delta t}{\lambda_*} = 0.8294 \frac{0.0017}{72.3701 \times 10^{-5}} = 1.9483\,\text{kg/mm}^2$$

in the case of BGA, and

$$\tau_{\max} = k_* \frac{\Delta\alpha\Delta t}{\lambda_*} = 0.6278 \frac{0.0017}{72.3701 \times 10^{-5}} = 1.4747\,\text{kg/mm}^2$$

in the case of CGA. Thus, the application of the low-modulus solder at the assembly ends (at about 6.6 % of its length) resulted in about 13 % relief in the maximum shearing stress, in the case of BGA, and in about 24 % relief in the case of CGA. With the yield stress in shear of 1.85 kg/mm^2 for the solder in the mid-portion of the assembly and 1.35 kg/mm^2 for the solder material at the peripheral portions, we conclude that the application of the CGA system in combination with a low modulus solder at the assembly ends might enable one to avoid inelastic strains in the solder. A further relief in the induced stress seems to be achievable by the appropriate selection of the bonding solders and by optimizing the size of the peripheral portions of the assembly, where low modulus solders are employed.

4 Conclusions

The following conclusions can be drawn from the carried out analysis:

- A simple, easy-to-use and physically meaningful predictive model is developed for the assessment of thermal stresses in a BGA or in a CGA with a low modulus solder material at the peripheral portions of the assembly.
- Application of such a design can lead to a considerable relief in the interfacial stresses, even to an extent that inelastic strains in the solder joints could be avoided. If this happens, the fatigue strength of the bond and of the assembly as a whole will be improved dramatically.
- Further work will include finite element analyses and experimental investigations.

References

1. J.R. Martin, R.A. Anderson, Compliant diaphragm material, U.S. Patent #4,837,068 (1989)
2. Z. Kovac et al., Compliant interface for semiconductor chip and method therefor, U.S. Patent #6,133,639 (2000)
3. E. Suhir, Electronic assembly having improved resistance to delamination, U.S. Patent #6,028,772 (2000)
4. E. Suhir, Device and method of controlling the bowing of a soldered or adhesively bonded assembly, U.S. Patent #6,239,382 (2001)
5. T.H. Di Stefano et al., Compliant microelectronic mounting device, U.S. Patent #6,370,032 (2002)
6. E. Suhir, Bi-material assembly adhesively bonded at the ends and fabrication method, U.S. Patent #6,460,753 (2002)
7. E. Suhir, Coated optical glass fiber, U.S. Patent #6,647,195 (2003)
8. Z. Kovac et al., Methods for making electronic assemblies including compliant interfaces, U.S. Patent #6,525,429 (2003)
9. E.C. Paterson et al., Mechanical highly compliant thermal interface pad, U.S. Patent #6,910,271 (2005)
10. Z. Kovac et al., Methods of making microelectronic assemblies including compliant interfaces, U.S. Patent #6,870,272 (2005)
11. R. Zeyfang, Stresses and strains in a plate bonded to a substrate: semiconductor devices. Solid State Electron. **14**, 1035–1039 (1971)
12. D. Chen, S.T. Cheng, T.D. Gerhardt, Thermal stresses in laminated beams. J. Thermal Stress. **5**, 67–84 (1982)
13. F.-V. Chang, Thermal contact stresses of Bi-metal strip thermostat. Appl. Math. Mech. **4**(3), 363–376 (1983)
14. J. Padovan, Anisotropic thermal stress analysis. Thermal Stress. I **1**, 143–262 (1986)
15. E. Suhir, Calculated thermally induced stresses in adhesively bonded and soldered assemblies, in *Proceedings of the International Symposium on Microelectronics*, ISHM, Atlanta, Georgia (1986)
16. E. Suhir, Stresses in Bi-metal thermostats. ASME J. Appl. Mech. **53**(3), 657–660 (1986)
17. E. Suhir, Die attachment design and its influence on the thermally induced stresses in the die and the attachment, in *Proceedings of the 37th Electrical and Computer Conference*, IEEE, Boston, MA, (1987) pp. 508–517
18. E. Suhir, An approximate analysis of stresses in multilayer elastic thin films. ASME J. Appl. Mech. **55**(3), 143–148 (1988)
19. A. Kuo, Thermal stresses at the edge of a bimetallic thermostat. ASME J. Appl. Mech. **56**, 585–589 (1989)
20. E. Suhir, Interfacial stresses in Bi-metal thermostats. ASME J. Appl. Mech. **56**(3), 595–600 (1989)
21. E. Suhir, Axisymmetric elastic deformations of a finite circular cylinder with application to low temperature strains and stresses in solder joints. ASME J. Appl. Mech. **56**(2), 328–333 (1989)
22. E. Suhir, B. Poborets, Solder glass attachment in Cerdip/Cerquad packages: thermally induced stresses and mechanical reliability, in *Electronic Components and Technology Conference, 40th, IEEE* (1990) pp. 1043–1052
23. J.W. Eischen, C. Chung, J.H. Kim, Realistic modeling of the edge effect stresses in bimaterial elements. ASME J. Electron. Packag. **112**(1), 16–23 (1990)
24. P.M. Hall et al., Strains in aluminum–adhesive–ceramic trilayers. ASME J. Electron. Packag. **112**(4), 288–302 (1990)
25. A.Y. Kuo, Thermal stress at the edge of a Bi-metallic thermostat. ASME J. Appl. Mech. **56**(3), 585–589 (1989)
26. C.A. Klein, Thermal stress modeling for diamond-coated optical windows, in *22nd Annual Boulder Damage Symposium*, Boulder, CO, (Oct 24–26, 1990) pp. 488–509
27. J.T. Gillanders, R.A. Riddle, R.D. Streit, I. Finnie, Methods for determining the mode I and mode II fracture toughness of glass using thermal stresses. ASME J. Eng. Mater. Technol. **112**, 151–156 (1990)
28. A.O. Cifuentes, Elastoplastic analysis of bimaterial beams subjected to thermal loads. ASME J. Electron. Packag. **113**(4), 355–358 (1991)
29. H.S. Morgan, Thermal stresses in layered electrical assemblies bonded with solder. ASME J. Electron. Packag. **113**(4), 350–354 (1991)

30. T. Hatsuda, H. Doi, T. Hayasida, Thermal strains in flip–chip joints of die-bonded chip packages, in *Proceedings of the EPS Conference*, San-Diego (1991)
31. E. Suhir, Mechanical behavior and reliability of solder joint interconnections in thermally matched assemblies, in *Proceedings of the 42nd Electronic Components and Technology Conference, IEEE*, San-Diego, CA (1992) pp. 563–572
32. J.H. Lau (ed.), *Thermal stress and strain in microelectronics packaging* (Van-Nostrand Reinhold, New York, 1993)
33. V. Mishkevich, E. Suhir, Simplified approach to the evaluation of thermally induced stresses in Bi-material structures, in *Structural analysis in microelectronics and fiber optics*, ed. by E. Suhir (ASME Press, New York, 1993), pp. 563–572
34. E. Suhir, Approximate evaluation of the elastic thermal stresses in a thin film fabricated on a very thick circular substrate. ASME J. Electron. Packag. **116**(3), 171–176 (1994)
35. E. Suhir, Approximate evaluation of the interfacial shearing stress in circular double lap shear joints, with application to dual-coated optical fibers. Int. J. Solids Struct. **31**(23), 3261–3283 (1994)
36. K.E. Hokanson, A. Bar-Cohen, Shear-based optimization of adhesive thickness for die bonding. IEEE Trans. Compon. Hybrids Manuf. Technol. **18**(3), 578–584 (1995)
37. E. Suhir, Solder materials and joints in fiber optics: reliability requirements and predicted stresses, in *Proceedings of the International Symposium on "Design and Reliability of Solders and Solder Interconnections"*, Orlando, FL (1997) pp. 25–33
38. E. Suhir, Thermal stress failures in microelectronics and photonics: prediction and prevention. Future Circuits Int. **5**, 20 (1999)
39. E. Suhir, Adhesively bonded assemblies with identical nondeformable adherends: predicted thermal stresses in the adhesive layer. Compos. Interface **6**(2), 62 (1999)
40. E. Suhir, Predicted stresses in a circular substrate/thin-film system subjected to the change in temperature. J. Appl. Phys. **88**(5), 2363–2370 (2000)
41. E. Carrera, An assessment of mixed and classical theories for the thermal stress analysis of orthotropic multilayered plates. J. Thermal Stress. **23**(9), 97–831 (2000)
42. Y. Gao, J.-H. Zhao, A practical die stress model and its applications in flip-chip packages, in *Proceedings of 7th Intersociety Conference on Thermal and Thermo-mechanical Phenomena in Electronic Systems*, Las Vegas, NV (May 23–26, 2000)
43. W.-R. Jong, M.-L. Chang, The analysis of warpage for integrated circuit devices. J. Reinf. Plast. Compos. **19**(2), 64–180 (2000)
44. E. Suhir, Analysis of interfacial thermal stresses in a tri-material assembly. J. Appl. Phys. **89**(7), 3685–3694 (2001)
45. J.-S. Bae, S. Krishnaswamy, Subinterfacial cracks in Bi-material systems subjected to mechanical and thermal loading. Eng. Fract. Mech. **68**(9), 1081–1094 (2001)
46. J.-S. Hsu et al., Photoelastic investigation on thermal stresses in bonded structures, in *SPIE Congrès Experimental Mechanics* (Beijing, 15–17 October 2001), vol 4537 (2002) pp. 170–173
47. H.B. Fan, M.F. Yuen, E. Suhir, Prediction of delamination in a Bi-material system based on free-edge energy evaluation, in *53-rd ECTC Proceedings* (2003) pp. 1160
48. Y. Wen, C. Basaran, An analytical model for thermal stress analysis of multi-layered microelectronics packaging, in *54-th ECTC* (2004) pp. 369–385
49. D. Sujan et al., Engineering model for interfacial stresses of a heated Bi-material structure with bond material used in electronic packages. IMAPS J. Microelectron. Electron. Packag. **2**(2) (2005)
50. E. Suhir, J. Nicolics, Analysis of a bow-free pre-stressed test specimen. ASME JAM **81**(11), 114502-1–114502-4 (2014)
51. E. Suhir, D. Ingman, Highly compliant bonding material and structure for micro- and opto-electronic applications, in *ECTC'06 Proceedings*, San Diego (May 2006)
52. E. Suhir, D. Ingman, Highly compliant bonding material and structure for micro- and opto-electronic applications, in *Micro- and opto-electronic materials and structures: physics, mechanics, design, packaging, reliability*, ed. by E. Suhir, C.P. Wong, Y.C. Lee (Springer, Berlin, 2007)
53. E. Suhir, M. Vujosevic, Interfacial stresses in a Bi-material assembly with a compliant bonding layer. J. Appl. Phys. D **41**, 115504 (2008)
54. E. Suhir, T. Reinikainen, On a paradoxical situation related to lap shear joints: Could transverse grooves in the adherends lead to lower interfacial stresses? J. Appl. Phys. D **41**, 115505 (2008)
55. E. Suhir, "Global" and "Local" thermal mismatch stresses in an elongated Bi-material assembly bonded at the ends, in *Structural analysis in microelectronic and fiber-optic systems, symposium proceedings*, ed. by E. Suhir (ASME Press, New York, 1995), pp. 101–105
56. E. Suhir, Predicted thermal mismatch stresses in a cylindrical Bi-material assembly adhesively bonded at the ends. ASME J. Appl. Mech. **64**(1), 15–22 (1997)
57. E. Suhir, Thermal stress in a polymer coated optical glass fiber with a low modulus coating at the ends. J. Mater. Res. **16**(10), 2996–3004 (2001)
58. E. Suhir, Thermal stress in a Bi-material assembly adhesively bonded at the ends. J. Appl. Phys. **89**(1), 120–129 (2001)
59. E. Suhir, Thermal stress in an adhesively bonded joint with a low modulus adhesive layer at the ends. J. Appl. Phys. **55**, 3657–3661 (2003)
60. E. Suhir, Interfacial thermal stresses in a Bi-material assembly with a low-yield-stress bonding layer. Model. Simul. Mater. Sci. Eng. **14**, 1421 (2006)
61. E. Suhir, L. Bechou, B. Levrier, Predicted size of an inelastic zone in a ball-grid-array assembly. ASME J. Appl. Mech. **80**, 021007-1–021007-5 (2013)
62. E. Suhir, A. Shakouri, Assembly bonded at the ends: Could thinner and longer legs result in a lower thermal stress in a thermoelectric module (TEM) design? ASME J. Appl. Mech. **79**(6), 061010-1–061010-8 (2012)
63. E. Suhir, On a paradoxical situation related to bonded joints: Could stiffer mid-portions of a compliant attachment result in lower thermal stress? JSME J. Solid Mech. Mater. Eng. (JSMME) **3**(7), 990–997 (2009)
64. E. Suhir, Thermal stress in a Bi-material assembly with a "piecewise-continuous" bonding layer: theorem of three axial forces. J. Appl. Phys. D **42**, 045507-1–045507-7 (2009)
65. E. Suhir, Adhesively bonded assemblies with identical nondeformable adherends and inhomogeneous adhesive layer: predicted thermal stresses in the adhesive. J. Reinf. Plast. Compos. **17**(14), 1588–1606 (1998)
66. E. Suhir, Adhesively bonded assemblies with identical nondeformable adherends and "piecewise continuous" adhesive layer: predicted thermal stresses and displacements in the adhesive. Int. J. Solids Struct. **37**, 2229–2252 (2000)